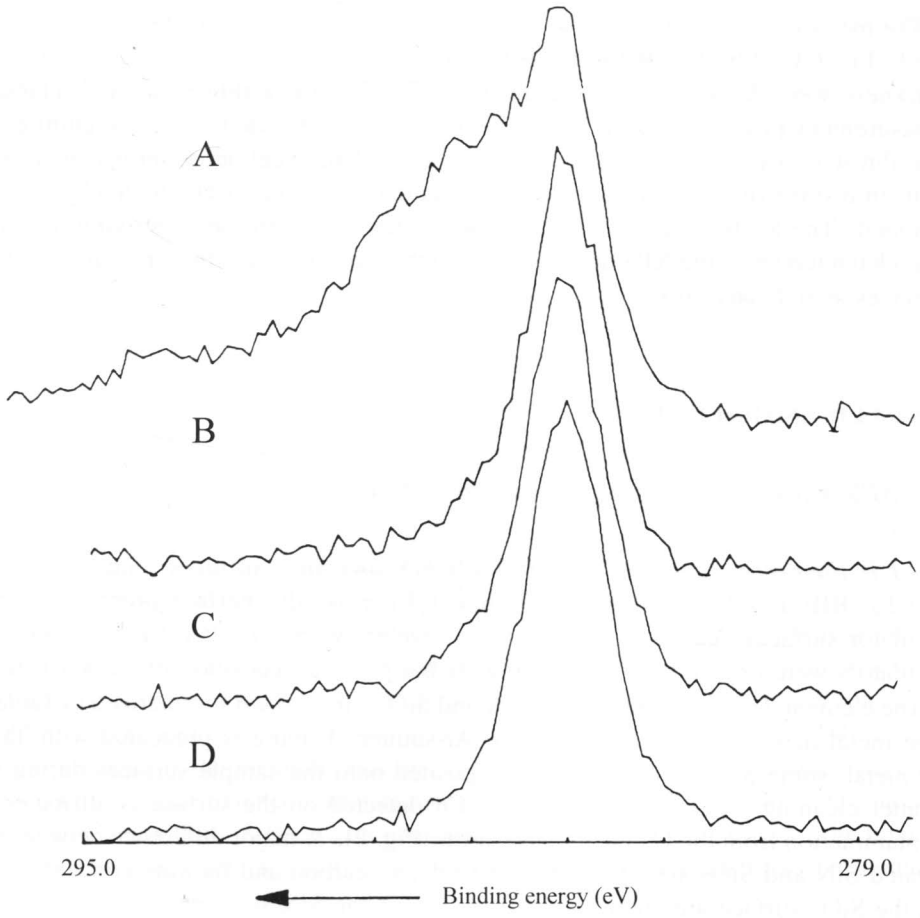

Figure 3. SiN and SiO_2 surface C1s XPS data after surface treatment. A) SiN CF_4–RIE, B) SiO_2 CF_4–RIE, C) SiN CF_4–RIE and Ar-sputter, and D) SiO_2 CF_4–RIE and Ar-sputter.

3.1.2. CF_4–RIE treatment of SiN. High resolution XPS analysis results of the CF_4–RIE treated SiN surface are listed in Table 4. The table lists the elements and the observed BEs, comparable BE data from the literature, their assignments and references. Figure 3 and Table 4 indicate that a fluorine-containing organic material is deposited on the SiN surface after exposure to CF_4–RIE. There are two F1s peaks, which are assigned to $-CF-$ or $-CF_3$ type organofluorine species. It should be noted that F1s associated with a fluoropolymer has BE between 689.3–690.8 eV [21]. The F1s BEs reported in Table 4 are significantly lower than these numbers, but are assigned to organic fluorine species based on the C1s data.

Fluorocarbon plasma etching and polymerization on Si-containing surfaces has been extensively studied by Coburn [33–35]. Oxygen is necessary for effective CF_4–RIE etching of SiO_2 or SiN [33, 34]. The oxygen removes surface carbon by forming volatile CO, CO_2 or COF_2 species on the surface [33, 34, 36] and making CF_4 polymerization impossible.

Table 4.
CF_4–RIE treated SiN surface characterization

Element	Observed BE (eV)	Literature BE (eV)	Literature assignment	References
Cls	285.0	285.0	$-CH_x$	[21–24]
	286.4	286.1	$-C-O$	[24]
		286.5	$-\mathbf{C}-CF_2-$	[23]
	287.5	287.5	$-\mathbf{C}-CF_3$	[25]
		287.6	$-C=O$ (ketone)	[26, 27]
		287.9	$-C=O$, $-CH_2-\mathbf{C}HF-CH_2-$	[23]
	288.9	288.9	$-C=O$, $-CHF-CHF-$	[23, 25]
	290.7	290.6	$-CF-$, $-CH_2-\mathbf{C}F_2-CH_2-$	[23, 28]
		290.8	$-\mathbf{C}F_2-CH_2-$	[21, 28]
	293.3	293.5	$-CF_3$	[21, 25, 28]
O1s	532.0	532.1	$-C-O-C-$	[12]
		532.5	$-Si-O-$	[29]
	533.2	533.4	$-C=O$	[12, 22]
F1s	687.4	687.3	$-CF-$	[30]
	688.7	688.4	$-CF_3$ ($Ni(OOCCF_3)_2$)	[31]
N1s	398.7	398.4	$-N-Si-O-$	[32]
	400.7	400.8	imide	[24]
Si2p	102.8	102.6	$-N-Si-O-$	[32]
	103.8	103.7	SiO_2	[29, 32]

Coburn and Kay [35] have shown that small amounts of nitrogen in fluorocarbon plasmas enhance the CF_4 polymerization rate on Si. The rate of CF_4 polymerization at the SiN surface may be enhanced due to nitrogen in the plasma from the SiN. The presence of nitrogen allows polymerization to compete successfully against the removal of carbon by oxygen release from the surface.

The conditions used to etch the SiN surface by CF_4–RIE cause CF_4 to polymerize on the SiN surface. However, some oxygen bonded to Si is detected on the SiN beneath the polymerized CF_4 as shown by the high BE of the Si2p peaks:

- 102.8 eV due to SiON [32], or SiO_x [31]
- 103.8 eV due to SiO_2 [32].

The presence of the SiO_2 at the SiN surface is indicated by the high BE Si2p peak, but the assignment of the lower BE Si2p peak is more difficult.

Two peaks are observed in the N1s spectrum: 398.7 eV, which could be assigned to $-N-Si-O-$(Si_3N_4 N1s is within 397.4–398.0 eV and Si2p 101.4–101.9 eV) [31, 32], and 400.7 eV. No assignment was made for the high BE N1s peak.

In summary, the SiN surface composition beneath the polymerized CF_4 appears to consists of SiO_2, SiON, and SiO_x, but not Si_3N_4.

3.1.3. CF_4–RIE treatment of SiO_2. High resolution XPS data of the CF_4–RIE treated SiO_2 surface are shown in Table 5. CF_4–RIE exposure of the PECVD SiO_2 results in Si2p at 104.1 eV assigned to SiO_2 species [31, 32]. The F1s has a doublet

Table 5.
CF_4–RIE treated SiO_2 surface characterization

Element	Observed BE (eV)	Literature BE (eV)	Literature assignment	References
Cls	285.0	285.0	$-CH_x$	[21–24]
	286.4	286.1	−C−O−	[24]
O1s	533.3	533.4	−C=O	[12, 22]
		532.5	−Si−O−	[29]
F1s	686.9	686.9	−Si−F	[37]
	687.9	687.3	−CF−	[30]
		687.8	Na_2SiF_6	[20]
Si2p	104.1	103.7	SiO_2	[29, 32]

at 686.9 eV and 687.9 eV, at a somewhat higher BE than suggested for a Si−F environment by Chuang *et al.* (686.0 eV) [20]. The highest BE C1s peak detected is at 286.6 eV, which can be interpreted as the α-carbon of $-CH_2-CF_2-$; however, a CF_2-group should have a C1s peak at 290.5 eV [21], which is not observed. A $-CH_2-CHF-\alpha$-carbon C1s peak at 285.9 eV and a −CHF− C1s peak at 288.0 eV have been reported [21]. Therefore, fluorine at the SiO_2 surface must be bonded to inorganic species in two different electronic environments. The O1s singlet is at 533.3 eV and must be due to oxygen in a SiO_2-type environment, though the O1s is at a higher BE than expected for SiO_2 [32] as is the Si2p peak. The two fluorine environments may be from fluorine in Si−F and/or Si−O−F groups.

In summary, the CF_4–RIE treated SiO_2 surface appears to consist of SiO_2, Si−F and/or Si−O−F species and ambient organic contamination.

3.1.4. CF_4–RIE and Ar-sputtering of SiN. After CF_4–RIE and Ar-sputtering XPS analyses for these studies are performed *ex-situ*. During fabrication of the metal-insulator structure shown in Fig. 1, the CF_4–RIE treated surfaces are exposed to ambient, while the Ar-sputtering is performed *in-situ* in the metal deposition tool. Ar-sputtering of the CF_4–RIE exposed SiN surface removes the fluoropolymer and the SiO_2 species as shown in Fig. 3C and Tables 3 and 6.

The C1s peak on the SiN surface after Ar-sputtering is attributed to ambient contamination. Small amounts of Cu, Ta or Cr on the Ar-sputtered SiN surfaces (Table 3) are redeposited from the peel release layer and the precoating in the Ar-sputter metallization chamber. The precoating of the metallization chamber affects the surface chemistry after Ar-sputter cleaning. After Ta precoating, the Si2p is a singlet at a BE of 102.4 eV; if the chamber was precoated with Cr, the Si2p spectrum contains a second peak at a BE of 100.7 eV (12 at-% of total Si concentration). The origin of this peak is not known. The BE range for metal silicide Si2p peak is 99.1–100.5 eV [31]. The corresponding metal BE in the silicide compounds overlaps with the elemental metal BE, except in the case of Ta [31] (Table 6). Since a low BE Cr2p peak is not observed, the silicide formation is not supported. O1s XPS data of the samples indicate that both Ta and Cr are in oxidized form, due to exposure to ambient prior to analysis. A second O1s peak is also found on the surface: in the Ta precoat

Table 6.
CF_4–RIE and Ar-sputter treated SiN surface characterization

Element	Observed BE (eV)	Literature BE (eV)	Literature assignment	References
Cls	285.0	285.0	$-CH_x$	[21–24]
	287.1	287.6	−C=O (ketone)	[26, 27]
O1s	531.4	530.6	Ta_2O_5	[31]
	532.7	532.5	−Si−O−	[29]
		533.4	−C=O	[12, 22]
N1s	398.3	398.4	−N−Si−O−	[32]
	397.1	396.7–398.8	Ta−N	[38]
		397.4–398.0	Si_3N_4	[31]
Si2p	102.4	101.9–103.0	−N−Si−O−	[29, 31, 32]
		102.0–102.7	−Si−O−	[31, 32]
Ta4f	24.5	24.0	TaO	[39]
	27.2	26.5–26.9	Ta_2O_5	[31, 39]
		27.0	$TaSi_2$	[31]

case the peak is at 532.7 eV suggesting perhaps a ketone, which is supported by the C1s data (C1s at 287.1 eV); in the Cr precoat case, the second O1s BE is 532.1 eV. Since the C1s on this sample lacks supporting evidence for ketone formation, it is suggested that this peak is due to SiO_x (Si2p BE $\approx$ 102.4 eV). Both SiN samples have two N1s peaks after the Ar-sputter treatment: one at 397.1 eV (Ta precoat) and the other at 396.5 eV (Cr precoat) assigned to Ta−N and Cr−N [31] environments, respectively. The second peak at 398.2 eV is assigned to SiON [32]. The presence of Si_3N_4 species cannot be ruled out since its N1s peak falls in between the two N1s peaks discussed (397.4–398.0 eV [31]); however, the Si2p peak BE of 102.4 eV is high for Si_3N_4 (101.4–101.9 eV [32]).

In summary, the CF_4–RIE and Ar-sputter treated SiN surface appears to consist of SiON, SiO_x, Ta and Cr oxides and nitrides, and ambient organic contamination.

3.1.5. CF_4–RIE and Ar-sputtering of SiO_2. High resolution XPS data of the CF_4–RIE and Ar-sputter treated SiO_2 surface are shown in Table 7. Ar-sputter exposure of the CF_4–RIE treated SiO_2 surfaces results in total removal of fluorine from the SiO_2 surface (Table 7). The Si2p peak is now at 103.3 eV, and is assigned to SiO_2 [31]. Oxygen 1s is a doublet with peaks at 532.8 eV and 531.3 eV for the Ta precoated chamber, and 532.5 eV and 530.9 eV for the Cr precoat. The higher BE O1s peak in both cases is due to SiO_2, and the lower BE peak is due to Ta-oxide or Cr-oxide [31]. The presence of Ta-silicide is not supported because of lack of a low BE Si2p peak (99.4–100.5 eV [31]).

The data for SiO_2 surfaces exposed to CF_4–RIE and Ar-sputtering suggest that the surfaces consist of SiO_2, some organic contamination due to ambient exposure, and redeposited metals (oxidized) due to peel release layer (Fig. 2) and the Ar-sputter chamber. Figure 4 summarizes the surface chemistry data for the SiO_2 and SiN surfaces exposed to both CF_4–RIE and Ar-sputter cleaning.

Table 7.
CF_4–RIE and Ar-sputter treated SiO_2 surface characterization

Element	Observed BE (eV)	Literature BE (eV)	Literature assignment	References
Cls	285.0	285.0	$-CH_x$	[21–24]
O1s	531.3	530.6	Ta_2O_5	[31]
	532.8	532.5	$-Si-O-$	[29]
Si2p	103.3	103.7	SiO_2	[29, 31, 32]
Ta4f	23.3	24.0	TaO	[39]
		21.8	Ta^0	[39]
	27.1	26.5–26.9	Ta_2O_5	[31, 39]
		27.0	$TaSi_2$	[31]

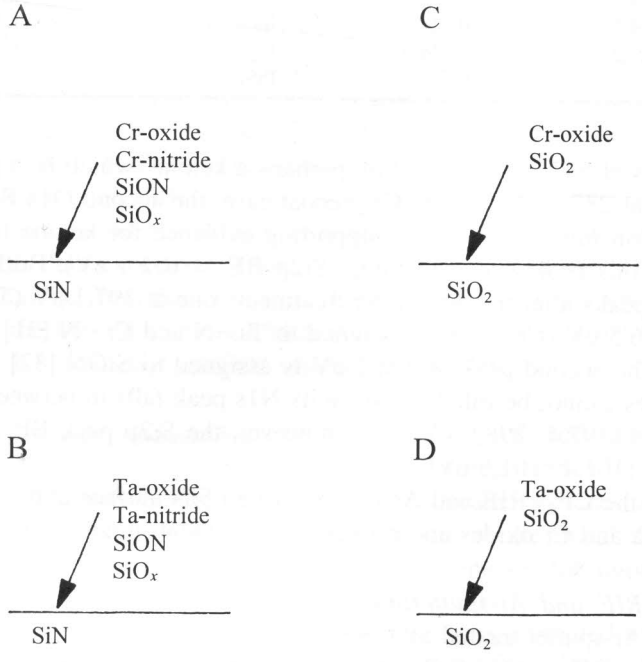

Figure 4. Summary of CF_4–RIE and Ar-sputter cleaned SiO_2 and SiN surface chemistries. A) Cr-precoated chamber, SiN surface, B) Ta-precoated chamber, SiN surface, C) Cr-precoated chamber, SiO_2 surface, and D) Ta-precoated chamber, SiO_2 surface. Carbon contaminants from the ambient are not shown.

3.2. Peel adhesion and locus of failure results

3.2.1. Peel adhesion results. The peel adhesion results for Ta/SiO_2, Ta/SiN, Cr/SiO_2, and Cr/SiN are compared in Fig. 5. Three peel experiments were done on each sample, with duplicate samples for the SiN interfaces.

Ordinarily peel strength data do not measure fundamental adhesion of a coating to the substrate [17]. The peel strength is the net result of energy-dissipating processes

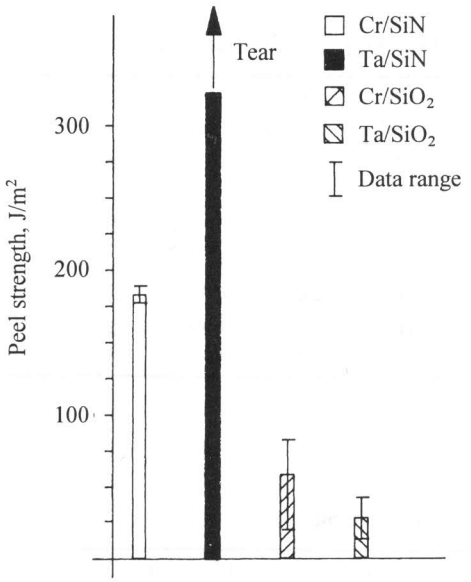

Figure 5. Ta and Cr peel strength to SiO_2 and SiN. The arrow in the Ta/SiN case indicates tearing of a 10 μm thick copper strip without peeling.

occurring during the peel process and the fundamental adhesion [17, 18, 40–43]. Loading of the interface at the peel crack tip affects the peel strength and the locus of failure [18, 44]. Loading (or phase angle [18, 43]) is relative to the ratio of tensile and shear stress intensity factors at the peel crack tip [18]. Thouless and Jensen [18] have shown that a change in the peel strength does not change the phase angle at a 90° peel angle. Therefore, although the measured Ta and Cr peel strengths (90° peel angle) between the SiN and SiO_2 systems differ significantly and consequently yield different peel strip radii of curvature, the phase angle (loading) at the peel crack tip has not changed. The mechanical properties of the peel strip (Cu on Ta or Cr) and the substrate (SiN or SiO_2 on Si-wafer) can be considered insignificantly different between samples tested, because Ta and Cr film thicknesses are only 2–3% of the Cu film thickness and SiN and SiO_2 film thicknesses are only a fraction of a percent of the of the 625 μm thick 5″ Si-wafer. Consequently, the peel test results are, to first order, not affected by any of the deposited thin films at the interphase.

Figure 5 shows that metal peel strength to SiN is stronger than it is to SiO_2. The Cu coated Cr peel strip has a peel strength of about 185 J/m^2 on SiN. The Cu coated Ta strip cannot be peeled from the SiN surface. When peeling is attempted cohesive failure (tearing) of the metal peel strip occurs. The Cr/SiO_2 peel strength is only 60 J/m^2; to peel Ta off SiO_2 requires only about 30 J/m^2. Ta and Cr adhesion to the PECVD SiO_2 are both extremely poor: the metal films are close to delaminating spontaneously. With such low peel strengths the differences between Ta and Cr peel adhesion to SiO_2 are insignificant.

The remainder of this paper focuses on peel locus of failure analyses as they relate to Fig. 5 data interpretation.